

# A methodology for spatial distribution of grain and voids in self compacting concrete using digital image processing methods

Okan Önal<sup>†</sup>, Gürkan Özden<sup>‡</sup> and Burak Felekoglu<sup>†‡</sup>

*Dokuz Eylul University, Department of Civil Engineering,  
Kaynaklar Yerleskesi, Buca-Izmir 35160, Turkey*

*(Received September 11, 2007, Accepted February 1, 2008)*

**Abstract.** Digital image processing algorithms for the analysis and characterization of grains and voids in cemented materials were developed using toolbox functions of a mathematical software package. Utilization of grayscale, color and watershed segmentation algorithms and their performances were demonstrated on artificially prepared self-compacting concrete (SCC) samples. It has been found that color segmentation was more advantageous over the gray scale segmentation for the detection of voids whereas the latter method provided satisfying results for the aggregate grains due to the sharp contrast between their colors and the cohesive matrix. The watershed segmentation method, on the other hand, appeared to be very efficient while separating touching objects in digital images.

**Keywords:** digital image processing algorithms; grain characteristics; segregation; void distribution; segmentation; watershed.

---

## 1. Introduction

Image processing is the process of extracting significant information from digitized images by transforming them into other images using various mathematical algorithms. In recent years, imaging and analysis techniques have become widely used tools for a variety of experimental observations. These techniques have enjoyed wide acceptance in many fields such as material, biomedical and geo sciences.

Research studies regarding determination of grain characteristics such as size, shape, orientation and spatial distribution either in sliced sections of cohesive materials or discrete aggregate samples using digital image analysis methods accelerated since 1980s (Michelland, *et al.* 1989, Yudhbir and Abedinzadeh 1991, Raschke and Hryciw 1997, Mora, *et al.* 1998, Kwan, *et al.* 1999). Some pioneering work, however, could be traced back to late 1960s (Saltykov 1967).

The majority of the above mentioned studies employed grayscale segmentation methods in the analysis of grain characteristics. In order to determine particle properties properly, some researchers have also used watershed segmentation to isolate touching grains (Ghalib and Hryciw 1999, Kim, *et al.* 2003). One alternative method called as the digital cutting method, which is based on the

---

<sup>†</sup> Graduate Research Assistant, Corresponding Author, E-mail: okan.onal@deu.edu.tr

<sup>‡</sup> Assistant Professor, E-mail: gurkan.ozden@deu.edu.tr

<sup>†‡</sup> Graduate Research Assistant, E-mail: burak.felekoglu@deu.edu.tr

threshold angle of contact wedge between grains has been proposed by Van den Berg, *et al.* (2002).

Digital image analysis data have been employed in the generation of finite element meshes (Yue, *et al.* 2003). It has been also possible to estimate other material characteristics such as permeability (Berryman and Blair 1986, Mowers and Budd 1996) and void ratio (Frost and Kuo 1996, Bhatia and Soliman 1990, Obaidat, *et al.* 1998) using digital image analysis methods.

Cohesive materials involving granular assemblies were also subject to digital image analysis (Yue and Morin 1996, Bisdorn and Schoonderbeek 1983, Ruzyla 1984, Pareschi, *et al.* 1990, Francus 1998). It has been demonstrated that size, shape, spatial distribution of grains in cohesive matrix such as rock and concrete specimens could be satisfactorily obtained using color and grayscale segmentation methods (Crabtree, *et al.* 1984, Soroushian, *et al.* 2003).

This study targets development of image analysis algorithms for the quantification of both grain and void distributions in artificially prepared and segregated samples of granular assemblies in cemented materials. The computer algorithms as presented here are fast enough and robust avoiding operator dependent errors in the stage of threshold determinations. This aspect of the study is especially reflected in the color segmentation, of which use has been found very beneficial while separating voids from the rest of the image. Trials for segmenting the voids in grayscale segmentation were not proved to be efficient since either void shapes could not be captured satisfactorily or the voids and small objects in the cohesive matrix were not detected during determination of the threshold levels. The color segmentation algorithm as employed in the code avoids such error sources. The codes can be easily modified and applied to other types of material investigations due to the universal toolbox functions being used. Although emphasis is given to toolbox algorithms of grayscale, color, and watershed segmentation, results of digital image analyses are also discussed.

## 2. Experimental work

Experimental work involved casting of artificial test specimens and establishment of the image acquisition system. In order to observe applicability of segmentation algorithms, two specimens were cast using basalt coarse aggregate, river sand and ordinary Portland cement and sliced horizontally into 12 pieces. One of these specimens served as the control sample where proportioning of the mixture has been made in such a manner that minimum segregation is allowed to take place along the specimen length. The other specimen, on the other hand, has been artificially segregated arranging mixture properties. The image acquisition system has been set using a digital camera and a stand, which was used to adjust height of the camera. Details of test specimens and the image acquisition system are given in the following.

### 2.1. Sample preparation

Two cylindrical specimens, 10 cm in diameter and 60 cm in height, were cast using ordinary Portland cement serving as the cementitious material. The well-known powder-type mix design method of self-compacting concrete (SCC) has been applied to the design and production of the specimen material (Okamura and Ouchi 1999). In order to increase the powder amount of the mix a C-type fly ash and limestone powder were used. Characteristics of the self-compacting mix proportions for the two specimens are given in Table 1. One should note that proportioning of self-

Table 1 SCC mix proportions

Material	Proportion	
	by weight per cubic meter, kg	by volume per cubic meter, l
cement	360	114
water	180	180
inert filler (limestone)	190	74
fly ash	140	62
sand	740	285
coarse aggregate	720	267
air content	-	10
admixture	12-36	10.9-32.7

compacting mixtures was the same except the admixture, a polycarboxylate type super plasticizer, of which proportion has been set as 3.3% and 10% of the cement weight in order to produce a non-segregating and an artificially segregated mixture, respectively.

The aggregate fraction of the mix consists of river sand and basalt type materials. The river sand of which specific gravity, minimum dry unit weight and water absorption characteristics were determined as 2.60, 14.6 kN/m<sup>3</sup> and 1.1%, respectively, constitutes finer portion of the aggregate fraction. The coarser portion of the aggregate, on the other hand, can be characterized as the crushed basalt material. The specific gravity, minimum dry unit weight and water absorption of this material were found as 2.7, 13.9 kN/m<sup>3</sup> and 0.3%, respectively. These two types of aggregates are combined together to yield the grain size distribution for the mix aggregate (Fig. 1).

In order to test the gray scale segmentation algorithm basalt has been selected as the coarse aggregate material due to its dark color so that a sharp contrast between the cohesive matrix and aggregate grains is ensured and a suitable environment for the preferred classification method of single-value thresholding technique for grain detection is formed. Samples were cured in lime-saturated water for 90 days. Following the curing period, samples were horizontally sliced into 12 pieces using a pit saw. In order to highlight voids on slice surfaces, sections have been plastered using jointing mortar and then sandpapered until the section surface reappeared. In this manner, voids have been filled with yellow

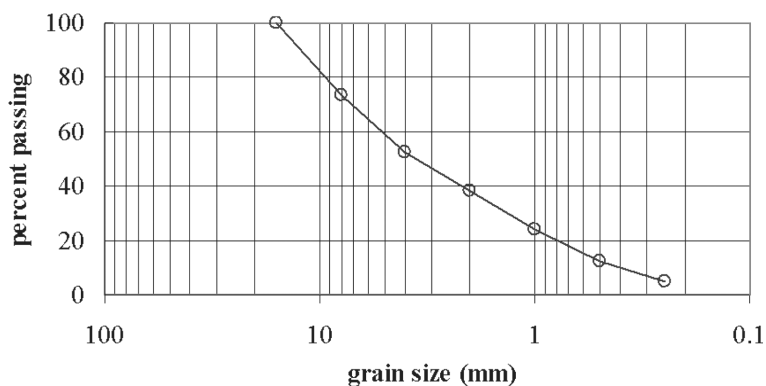


Fig. 1 Grain size distribution of the mix aggregate

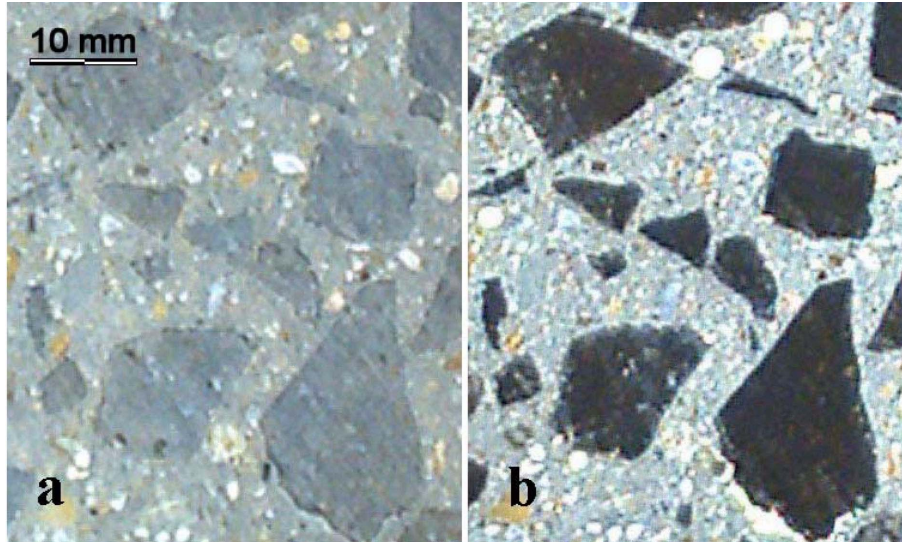


Fig. 2 Surface preparation of sliced sections prior to image capturing (a) unpolished (b) sand papered and polished

mortar, which can be detected by means of color segmentation techniques. Finally, sections have been polished to differentiate the coarse aggregate from the cohesive matrix (Fig. 2).

## 2.2. Image acquisition system

The success of digital image processing operation greatly depends on the quality of the captured image. Illumination conditions of sample and resolution of the image both influence outcomes of the operations directly. In the current study, a video camera with a high sensitive charged-coupled-device (CCD) sensor has been used. The camera (Philips ToUcam Pro II) has the capability of acquiring pictures with a snapshot resolution of 1.2 million-picture elements. The pictures are transferred directly via USB connection into a Pentium based personal computer without the need of a frame grabber board. Image capturing hardware uses its own twain interface allowing manual control of brightness-contrast, gamma and saturation, white balance and exposure values.

Since the surfaces of the samples are polished, diffuse illumination has been used to avoid the blazes of the nearby additional light sources, which would otherwise cause erroneous results during the analysis phase. The camera has been mounted in a photographic stand allowing the user to adjust the height to obtain a sufficiently large measurement area on the sample tray.

## 3. Image acquisition

Image acquisition has been performed via the twain interface of the camera with a resolution of 1290\*960 square pixels creating a field view of 147\*110 mm. Captured data have been kept in disk as an uncompressed image file format (BMP) since depending on the degree of compression, information regarding sharpness and spectral contrast across boundaries is especially lost (Russ

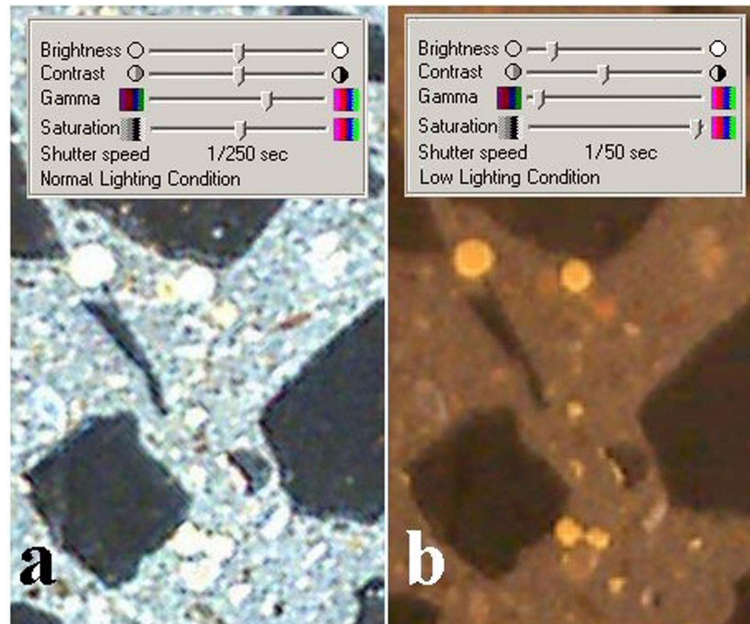


Fig. 3 Camera adjustments (a) for grain and (b) for void detection

1998). Two different sets of preprocessing adjustments in the twain interface have been applied for grain and void detection. For grain detection, brightness, contrast, gamma and saturation values have been set to intermediate values in order to extract grains from the rest of the image. It may be noticed in Fig. 3a that detection of the grains appears to be a relatively easy task due to the black color of the grains. However situation is different for voids appearing as white and bright spots in the cohesive matrix resulting in RGB values closer to those of the matrix (Fig. 3b). In order to ensure the separation of the voids and the background, their pixels values have been stretched by means of brightness and gamma adjustments. Since the void detection is based on color segmentation, saturation value has been set to its highest value to highlight the yellow pixels (Fig. 3b). For the void detection, image acquisition has been performed for the same slices in low lighting condition with a relatively lower shutter speed to avoid interference of the colors. It appeared that default imaging parameters of the camera were satisfactory for grain detection using gray scale segmentation whereas adjustment of the saturation parameter to its highest value was essential for the detection of void color during color segmentation. Proportioning of shutter speed, brightness, contrast and gamma values has been made based on visual inspection of the raw images so that void shapes are better separated from the rest of the image.

#### 4. Image processing

Image processing involved grayscale, color and watershed segmentation. The grayscale segmentation was employed in the determination of segregation of grains in the soft cohesive matrix of artificial segregated SCC sample whereas the color based segmentation was utilized for the detection of voids within the specimens. The watershed segmentation was used in order to isolate touching

grains and voids prior to the determination of their spatial distribution and shape characteristics. The toolbox of a mathematical analysis software package was employed in image processing M-files of the digital image analysis algorithms (Mathworks 2005).

#### 4.1. Grayscale segmentation

Captured images in RGB colors have been processed as multidimensional arrays. A transformation into grayscale images has been made eliminating the hue and saturation information while retaining the luminance, reducing the image into an 8-bit intensity one (Fig. 4a) with element values ranging 0 to 255. Particle analysis requires conversion of the captured image into a binary image following a contrast stretching transformation step (Fig. 4b), which is necessary to make grain shapes more visible. The transformation process consists of a piecewise linear function, which increases the dynamic range of the gray levels. The image is then thresholded in order to filter out the cohesive matrix from the rest of the picture obeying the methodology suggested by Otsu (1979). This method works on the gray levels of the image (Fig. 4b) by minimizing the intra-class variance of the black and white pixels. Resulting binary image of this step is given in Fig. 4(c). The white spots, appearing within the coarse grains probably result from non-uniform illumination or noise of various sources (environmental, transmission, etc). They were eliminated using a morphological operation as shown in Fig. 4(d). This was made by first finding the pixels that were not connected to its neighbors according to the eight adjacency pixel relationship (Gonzalez and Woods 2002) and then removing them from the image. This process eliminated noisy pixels enclosed in the coarse grains. The same technique was used for the elimination of finer aggregates in the cohesive matrix using the negative of the image as shown in Figs. 4(e). The touching grains in the final processed image were separated using the watershed segmentation as explained later in the text.

#### 4.2. Color segmentation

Color segmentation has been performed using  $L^*a^*b^*$  color space for the determination of voids

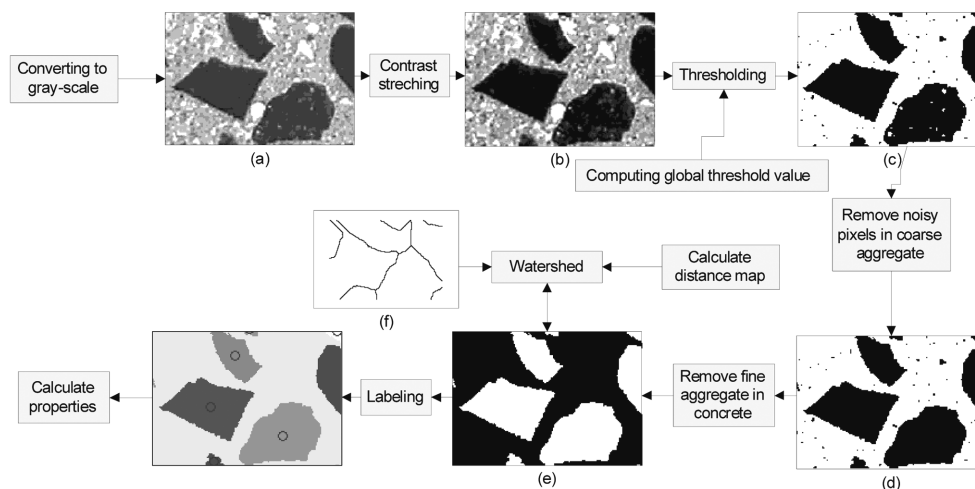


Fig. 4 Image processing flow chart of coarse grain detection by gray scale segmentation

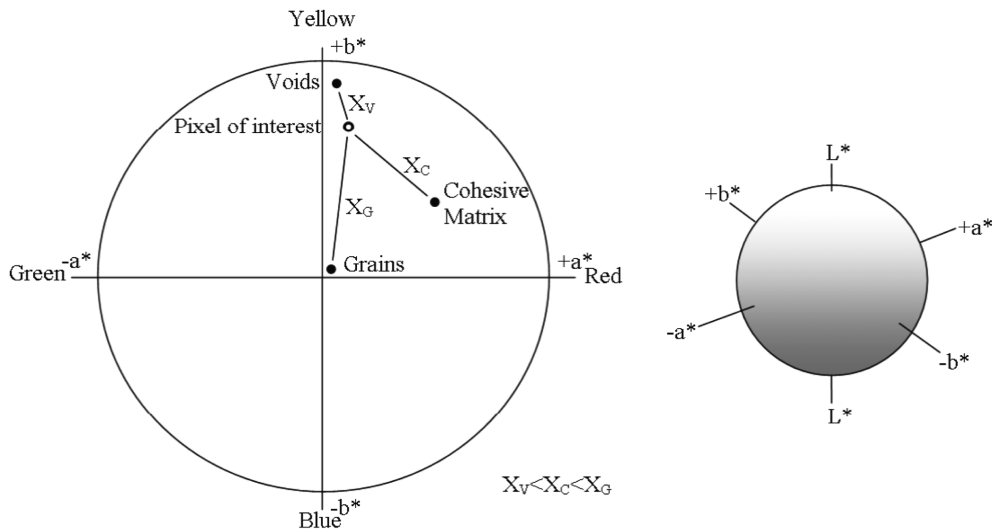


Fig. 5 The L\*a\*b\* color space model in color segmentation

in 2-D sections. The L\*a\*b\* color space model (Robertson 1997) has been introduced as a device independent color model enabling quantification of visual differences in any digitized image since influence of lighting conditions could be easily normalized in this space. The L\*a\*b color space consists of the luminosity ‘L\*’ or brightness layer, the chromaticity layer ‘a\*’ indicating the location of the color along the red-green axis, and the chromaticity layer ‘b\*’ indicating where the color falls along the blue-yellow axis (Fig. 5). During color segmentation, therefore, captured images were transformed into L\*a\*b\* space firstly.

It has been necessary to select only specific colors in the original image so that color segmentation could be performed satisfactorily without increasing computational effort and complexity of the algorithm. This has been made visually depending on the appearance of the original image. Two tones of yellow and gray colors were selected for the voids and the cohesive matrix, respectively. Such a two-tone definition was made in order to avoid erroneous segmentation

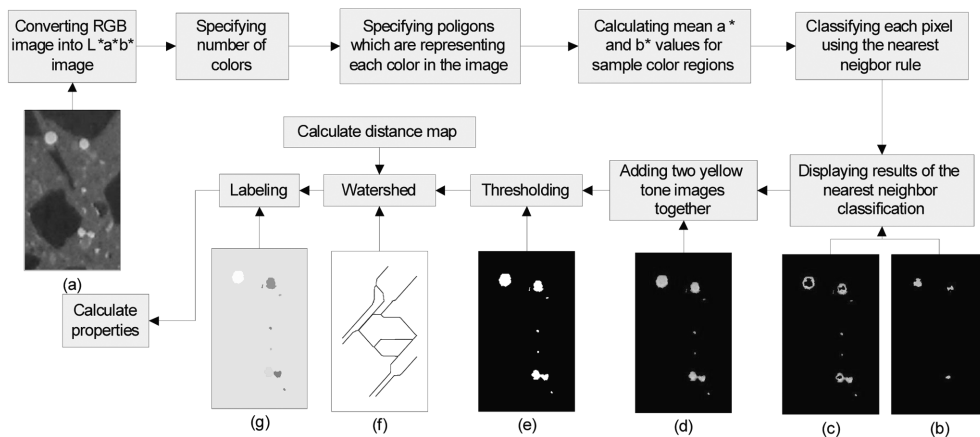


Fig. 6 Image processing flow chart of void detection by color segmentation

since color transition from the voids to the cohesive matrix in captured images takes place gradually. The grain objects, on the other hand, were related to the black color.

Five sample regions consisting of small triangles were generated on the image. Each sample region has been assigned one of the specified colors. The average  $a^*b^*$  values of pixels within the sample regions were calculated in the  $L^*a^*b^*$  color space. Color classification is made based on the closest Euclidian distance of each pixel to these average values. This procedure is also illustrated in Fig. 5. Following color segmentation two tones of the yellow color that were detected in the images have been added together and thresholded to form the resulting image, which has become ready for watershed segmentation where touching voids are separated. The flow chart diagram of the color segmentation process for void detection is given in Fig. 6.

#### 4.3. Watershed segmentation

A frequent problem encountered in the analysis of digital images is the objects that are in contact. Such contacts avoid one-by-one analysis of individual objects. In order to measure the size and

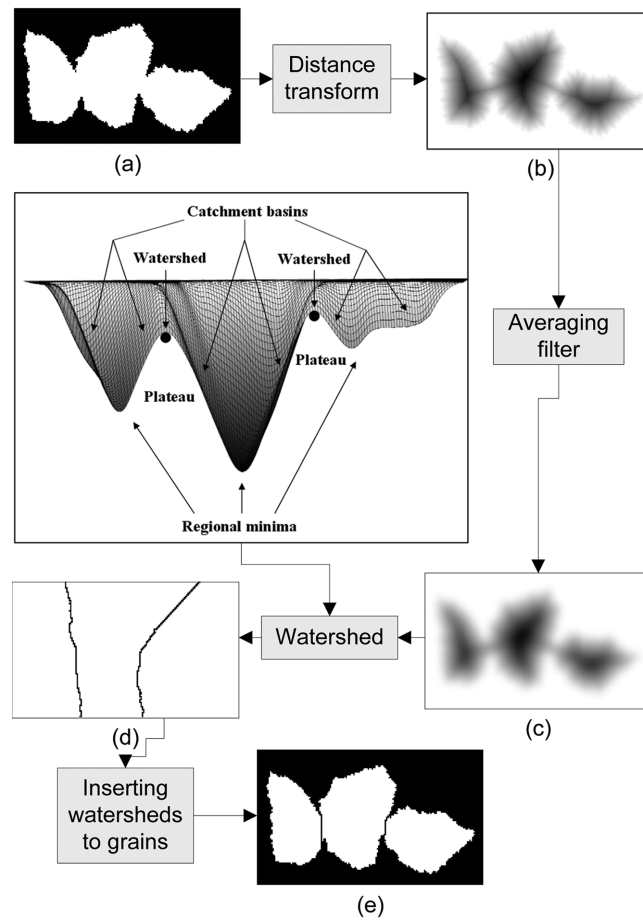


Fig. 7 Watershed segmentation algorithm tree

shape of these objects, sections that are in contact should be separated. It appears that the watershed segmentation algorithm originally developed by Beucher and Lantuejoul (1979) and then improved by Vincent and Soille (1991) is the most preferred technique for grain size or grain distribution type problems. Watershed segmentation requires grayscale images as topological surfaces, whose catchment basins are the objects to be identified (Gonzales, *et al.* 2004). A three-dimensional illustration of topological surface generation is shown in Fig. 7. The topological surface can be generated with a process called distance transform, which calculates the Euclidian distances from each pixel to the nearest black pixel (Fig. 7b). Results of the method, however, may be highly influenced by the presence of irregular boundaries and interior holes. Besides, lack of a minimum in the ridge of the Euclidian distance map may cause erroneous segmentations of the grains (Russ 1998). Since the distance map consists of numerous local catchment basins and watershed lines, application of watershed algorithm results in over segmentation of the objects. This effect, however, may be overcome by means of a multidimensional image-filtering algorithm, which eliminates local watershed lines generating a smoothed image as shown in Fig. 7(c). Following the smoothing stage of watershed application, separation lines along the contact points of the grains and voids are obtained as shown in Fig. 7(d), which is superimposed on the original binary image (Fig. 7a) to come up with the segmented image (Fig. 7e). The generation of a separation line may be further explained by the help of the flooded basins analogy where the line passing through the center of the plateau formed by watersheds between two neighboring catchment basins is considered as the dividing border as soon as the gradually increasing water levels in the basins finally form a single water level when they get into contact at the center of the plateau.

### 5. Image analysis

The image segmentation (i.e. segmented grains or voids in Fig. 4e and Fig. 6e) is followed by the characterization of the regions. The sectional area and the centroid for each grain and void were defined for the problem of interest. A region map, where labels are assigned to pixels has been generated using the eight adjacency pixel relationship (Fig. 8). This process has been used to improve the accuracy near the corners and edges of the regions. Quantitative information about the objects could then be obtained examining their regional properties using various algorithms in the region map. For instance, grain and void size distribution of the objects in a certain slice of any geomaterial can be easily acquired since number of corresponding pixels for each region is already known. Area information can be gathered either in terms of percent of the total pixel area or numerical value of the physical quantity provided that a suitable scale is available in the image.

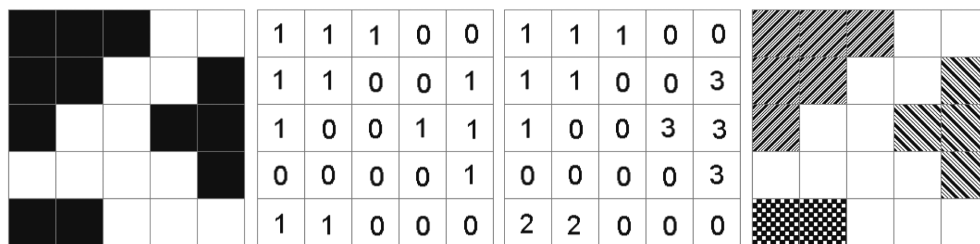


Fig. 8 Binary image, binary matrix, label matrix and labeled images

## 6. Results and discussions

An experimental study has been pursued parallel to the development of the image analysis algorithms so that their performances could be assessed using images of the sliced sections of the test samples. Images were analyzed according to the above given methodology. Analysis results pertinent to the quantification of the slice images are presented and discussed as in the following.

Since one of the artificially prepared samples was intentionally segregated by means of additives, image analysis algorithms were expected to capture non-uniform grain and void distribution along sample length. This aspect of the tested materials is shown in Fig. 9 where digital images of the upper faces of the slices along sample length can be seen. Non-uniform grain and void distributions of the segregated sample are visible in Figs. 9b and 9d, respectively. The other sample, on the other hand, exhibits quite uniform distribution since the cohesive matrix of this sample was able to provide enough resistance to avoid segregation (Figs. 9a and 9c).

The non-uniformity of grain and porosity distribution, however, can be best judged using results of digital image analyses. Ratio of the total grain area to the surface area of the slice (area ratio) is plotted with respect to sample length in Fig. 10a. Area ratios for the segregated and non-segregated samples were computed as 0.25 and 0.26, respectively. These values are quite close to each other and do not yield much information regarding the influence of the cohesive matrix characteristics on segregation. Instead, standard deviation of the data better demonstrates such an effect. This parameter has been calculated as 0.183 for the segregated sample whereas it has been found as 0.041 for the non-segregated one. Similar evaluations can be made for the porosity distribution

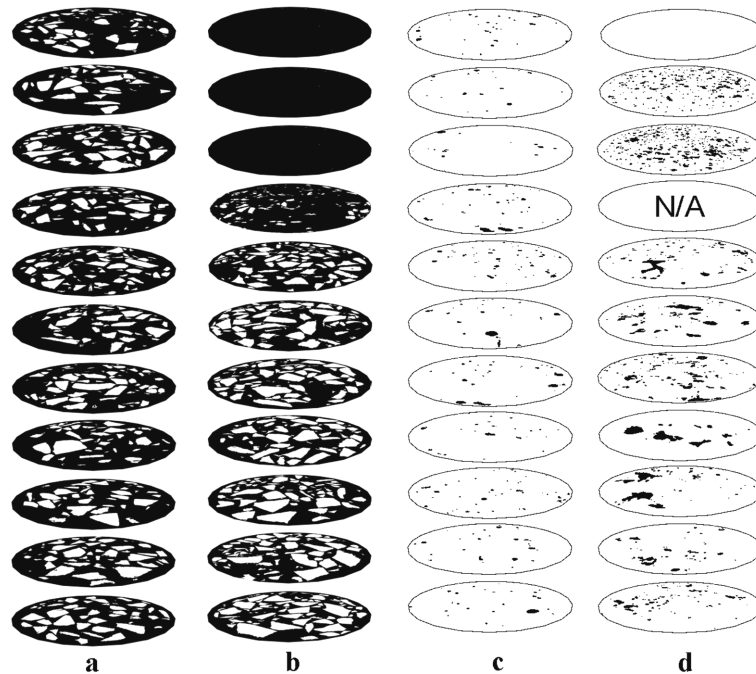


Fig. 9 (a) Grain distribution for the non-segregated specimen, (b) grain distribution for the segregated specimen, (c) void distribution for the non-segregated specimen, (d) void distribution for the segregated specimen

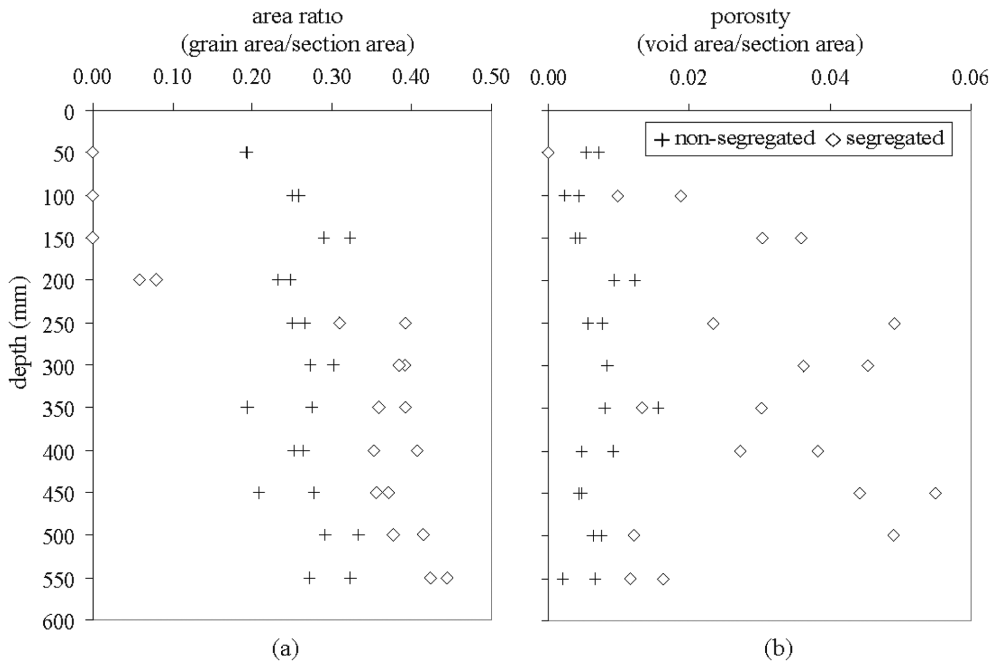


Fig. 10 (a) Grain area ratio variation and (b) porosity variation along specimen length

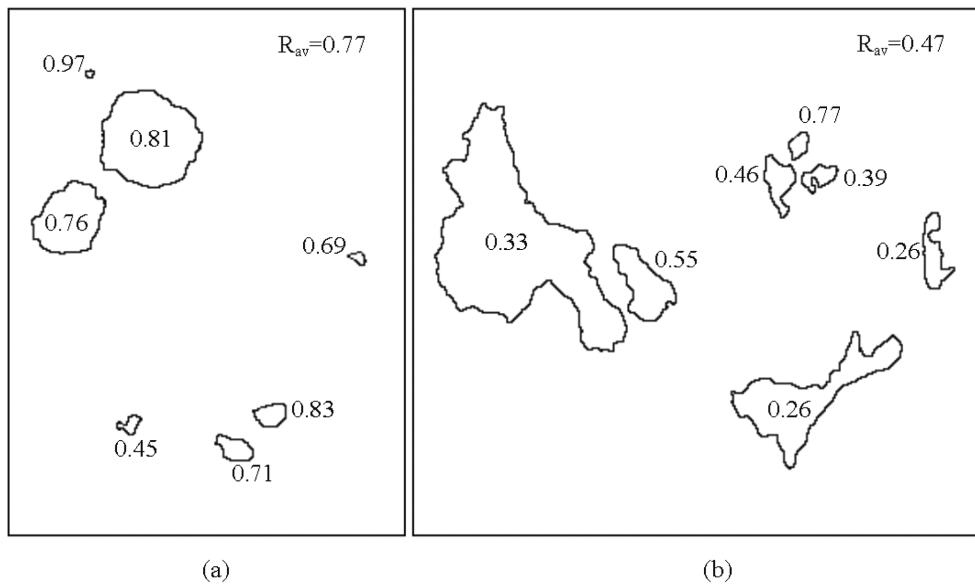


Fig. 11 Void shape characteristics in (a) non-segregated and (b) segregated specimens

along sample length as shown in Fig. 10(b). Porosity is defined as the ratio of the void area to the total section area in this figure. Random distribution of the porosity in the segregated sample is remarkable. The non-segregated sample, however, exhibited more uniform porosity distribution. Respective values of average porosity and its standard deviation have been found as 0.0067 and

0.0032 for the non-segregated sample. Same parameters happened to be 0.027 and 0.0167 for the segregated sample indicating higher void volume and its non-uniform distribution. Note that it was even not possible to compute porosity for the top fourth image of the segregated sample due to excessive disintegration of the fine river sand under dynamic impact of the blade during slicing operation. Same effect did not exist for coarser basalt grains.

It has been observed that cohesive matrix characteristics control void shape as well. A closer look to the slice images revealed that voids of the segregated sample are more rounded compared with those of the non-segregated sample. An example to this observation can be given from the image of the eighth slice from the top of the sample (i.e. at 400 mm). An enlarged portion of this image is presented in Fig. 11. The image on the left hand side (i.e. Fig. 11a) belongs to the non-segregated sample whereas Fig. 11(b) is from the segregated one. It is clearly seen that shapes of the voids in the non-segregated sample are more circular than those in the segregated one. This characteristics of the voids can be numerically expressed using the roundness parameter,  $R$ , which is defined as  $R=(4 \cdot \pi \cdot \text{area})/(\text{perimeter})^2$  where area and perimeter are given in pixels for each void. The roundness ratio equals to unity for a perfectly circular void. The roundness values are typed next to each void in Figs. 11(a) and 11(b). One should note that the average roundness value on area basis ( $R_{av}=\sum R_i \cdot A_i / \sum A_i$ ) for the segregated sample is found as 0.77 being closer to unity when compared with that of the image of the non-segregated sample containing more irregularly shaped voids thereby yielding an average roundness value of 0.47.

## 7. Conclusions

The study demonstrated that digital image analysis subroutines readily available in commercial mathematical analyses software packages could be easily organized to form problem specific algorithms. Although the performance of the algorithms developed herein was tested on the images of SCC samples, they are equally applicable to the investigation of geomaterials such as rock with breccias, sandy and gravelly clay samples. Results of the image analyses showed that image analysis methodology as presented here was able to demonstrate that characteristics of the cohesive matrix would have considerable influence on the distribution of coarser grains and voids in SCC samples. The more irregularly shaped voids and random distribution of the porosity in segregated samples may be attributed to the additives used to trigger segregation in concrete samples. It has been noticed that color segmentation would be especially helpful if several different objects with varying colors exist in the original image. The gray scale segmentation, itself, could not fully differentiate the voids from the cohesive matrix. The color segmentation, on the other hand, generates several object layers and can fulfill this task much more effectively.

## References

- Berryman, J. G. and Blair, S. C. (1986), "Use of digital image analysis to estimate fluid permeability of porous material: Application of two-point correlation functions", *J. Applied Physics*, **60**(6), 1930-1938.
- Beucher, S. and Lantuejoul, C. (1979), "Use of watersheds in contour detection", *Proceedings of the international Workshop on Image Processing, Real-Time Edge and Motion Detection/Estimation, Rennes, France*.

- Bhatia, S. K. and Soliman, A. F. (1990), "Frequency distribution of void ratio of granular materials determined by an image analyzer", *Soils and Foundations*, **30**(1), 1-16.
- Bisdorn, E. B. A. and Schoonderbeek, D. (1983), "The characterization of the shape of mineral grains in thin sections of soils by Quantimet and BESI", *Geoderma*, **30**, 303-322.
- Crabtree, S. J., Ehrlich, Jr. R. and Prince, C. (1984), "Evaluation of strategies for segmentations of reservoir rocks", *Computers Vision, Graphics and Image Processing*, **28**(1), 1-18.
- Francus, P. (1998). "An image analysis technique to measure grain-size variation in thin sections of soft clastic sediments", *Sedimentary Geology*, **121**, 289-298.
- Frost, J. D. and Kuo, C.-Y. (1996), "Automated determination of the distribution of local void ratio from digital images", *Geotechnical Testing J.*, **19**(2), 107-117.
- Ghalib, A. M. and Hryciw, R. D. (1999), "Soil particle size distribution by mosaic imaging and watershed analysis", *J. Comput. Civ. Eng.*, **13**(2), 80-88.
- Gonzales, R. C. and Woods, R. E. (2002), *Digital Image Processing*, Pearson Prentice Hall, New Jersey.
- Gonzales, R. C., Woods, R. E. and Eddins, S. L. (2004), *Digital Image Processing Using MATLAB*, Pearson Prentice Hall, New Jersey.
- Kim, H., Haas, C. T., Rauch, A. F. and Browne, C. (2003), "3D image segmentation of aggregates from laser profiling", *Comput.-Aid. Civ. Infrastr. Eng.*, **18**, 254-263.
- Kwan, A. K. H., Mora, C. F. and Chan, H. C. (1999), "Particle shape analysis of coarse aggregate using digital image processing", *Cement Concrete Res.*, **29**(9), 1403-1410.
- Mathworks (2005), *MATLAB Technical Computing Language Version 7 and Image Analysis Toolbox Version 4.2*, Natick, MA.
- Michelland, S., Schiborr, B., Coster, M., Mordike, B. L. and Chermant, J. L. (1989), "Size distribution of granular materials from unthresholded images", *J. Microscopy* **156**(3), 303-311.
- Mora, C. F., Kwan, A. K. H. and Chan, H. C. (1998), "Particle size distribution analysis of coarse aggregate using digital image processing", *Cement Concrete Res.*, **28**(6), 921-932.
- Mowers, T. T. and Budd, D. A. (1996), "Quantification of porosity and permeability reduction due to calcite cementation using computer-assisted petrographic image analysis techniques", *Bulletin of the American Association of Petroleum Geologist*, **80**(3), 309-322.
- Obaidat, M. T., Al-Masaeid, H. R., Gharaybeh, F. and Khedaywi, T. S. (1998), "An innovative digital image analysis approach to quantify the percentage of voids in mineral aggregates of bituminous mixtures", *Canadian J. Civ. Eng.*, **25**(6), 1041-1049.
- Okamura, H. and Ouchi, M. (1999), "Self-compacting concrete, development, present use and future", *Proceedings of the First International RILEM Symposium on Self-Compacting Concrete*, Ed.: Rilem Publications s.a.r.l., Stockholm, pp. 3-14.
- Otsu, N. (1979), "A threshold selection method from gray-level histograms", *IEEE Transactions on Systems, Man, and Cybernetics*, **9**(1), 62-66.
- Pareschi, M.T., Pompilio, M. and Innocenti, F. (1990), "Automated evaluation of volumetric grain-size distribution from thin-section images", *Comput. Geosci.*, **16**(8), 1067-1084.
- Raschke, S. A. and Hryciw, R. D. (1997), "Grain-size distribution of granular soils by computer vision", *Geotechnical Testing J.*, **20**(4), 433-442.
- Robertson, A. R. (1997), "The CIE 1976 color difference formulae", *Color Research and Application*, **2**, 7-11.
- Russ, J. C. (1998), *The Image Processing Handbook*, 3<sup>rd</sup> edn., CRC Press LLC in cooperation with IEEE Press, Boca Raton, FL.
- Ruzyla, K. (1984), "Characterization of pore space by quantitative image analysis", *59<sup>th</sup> Annual Technical Conference and Exhibition*, Society of Petroleum Engineers of AIME, Houston, pp. 13.
- Saltykov, S. A. (1967), "The determination of the size distribution of particles in an opaque material from a measurement of the size distribution of their sections", *Proceedings of the Second International Congress for Stereology*, Springer, New York, pp. 163.
- Soroshian, P., Elzafraney, M. and Nossioni, A. (2003), "Specimen preparation and image processing and analysis techniques for automated quantification of concrete micro cracks and voids", *Cement Concrete Res.*, **33**(12), 1949-1962.
- Van den Berg, E. H., Meesters, A. G. C. A., Kenter, J. A. M. and Schlager, W. (2002), "Automated separation of

- touching grains in digital images of thin sections”, *Comput. Geosci.*, **28**(2), 179-190.
- Vincent, L. and Soille, P. (1991), “Watersheds in digital spaces: an efficient algorithm based on immersion simulations”, *IEEE Transactions of Pattern Analysis and Machine Intelligence*, **13**(6), 583-598.
- Yudhbir, J. and Abedinzadeh, R. (1991). “Quantification of particle shape and angularity using the image analyzer”, *Geotech. Testing J.*, **14**(3), 296-308.
- Yue, Z. Q. and Morin, I. (1996), “Digital image processing for aggregate orientation in asphalt concrete mixtures”, *Canadian J. Civ. Eng.*, **23**(2), 480-489.
- Yue, Z. Q., Chen, S. and Tham, L. G. (2003), “Finite element modeling of geomaterials using digital image processing”, *Comput. Geotech.*, **30**(5), 375-397.

CC